Journal of Inflammation Research

Dovepress
Taylor & Francis Group

Open Access Full Text Article

ORIGINAL RESEARCH

Integration of Multi-Omics and Network Pharmacology Analysis Reveals the Mechanism of Qingchang Huashi Jianpi Bushen Formula in Repairing the Epithelial Barrier of Ulcerative Colitis

Yulai Fang[1,*], Shichen Min[2,*], Yuguang Wu[2], Feng Xu[2], Hongxin Chen[2], Yanan Li[2], Yizhou Lu[2], Jingyi Hu[1], Lei Zhu[1], Hong Shen[1]

[1]Digestive Disease Research Institute, Affiliated Hospital of Nanjing University of Chinese Medicine, Nanjing, People's Republic of China; [2]First Clinical Medical College, Nanjing University of Chinese Medicine, Nanjing, People's Republic of China

*These authors contributed equally to this work

Correspondence: Hong Shen; Lei Zhu, Digestive Disease Research Institute, Affiliated Hospital of Nanjing University of Chinese Medicine, Nanjing, People's Republic of China, Email Shenhong999@njucm.edu.cn; zhulei5100@njucm.edu.cn

Purpose: Derivation of Qingchang Huashi formula, named Qingchang Huashi Jianpi Bushen (QCHS_JPBS) formula, has shown significant therapeutic effect on patients with ulcerative colitis (UC). In this study, the potential mechanism of QCHS_JPBS formula in repairing mucosal damage was explored from the perspective of intestinal stem cell (ISCs) differentiation, and potential targets of the QCHS_JPBS formula to improve UC were predicted using network pharmacology analysis.

Methods: The therapeutic efficacy of QCHS_JPBS formula was evaluated in a mouse model of 2.5% dextran sulfate sodium (DSS) induced colitis. The effect of this formula on the ISC differentiation was evaluated using tissue transmission electron microscopy, immunofluorescence, and RT-qPCR. The cecal contents were subjected to 16s RNA sequencing analysis and non-target metabolomics analysis using LC-MS/MS. The fecal microbiota transplantation method verified the essential role of gut microbiota in promoting ISC differentiation and repairing mucosal damage.

Results: The results indicated that QCHS_JPBS formula suppressed the inflammatory response and repaired the damaged intestinal epithelial barrier in DSS-induced colitis mice. QCHS_JPBS formula promoted ISC differentiation, particularly in the direction of goblet cells. QCHS_JPBS formula restored gut dysbiosis and regulated metabolic disorders in DSS-induced colitis mice. And then, the results of fecal microbiota transplantation indicated that QCHS_JPBS formula promoted differentiation of intestinal stem cells to repair mucosal damage through gut microbiota. Finally, a total of 79 active ingredients of QCHS_JPBS formula were identified based on LC-MS analysis and EGFR, STAT3, SRC, AKT1, and HSP90AA1 were considered as potential therapeutic UC targets of QCHS_JPBS formula based on network pharmacology analysis.

Conclusion: The present study demonstrated that QCHS_JPBS formula promoted the differentiation of ISCs through gut microbiota to repair the damaged intestinal epithelial barrier in UC mice.

Keywords: qingchang huashi jianpi bushen formula, ulcerative colitis, intestinal stem cells, epithelial barrier, gut microbiota, network pharmacology

Introduction

Ulcerative colitis (UC), classified as an inflammatory bowel disease, is a chronic relapsing inflammatory disease characterized by uncontrolled inflammation and destruction of the epithelial structure of the intestine.[1] Nevertheless, the mechanisms involved in the pathogenesis of UC are unknown, which may involve environmental factors, genetic susceptibility, immune dysfunction, and microbial imbalance.[2] Currently, the primary drugs used clinically for the therapy of UC include salicylates, corticosteroids, and immune and biological agents. However, due to the side effects

Received: 20 December 2024
Accepted: 30 April 2025
Published: 12 May 2025

of these drugs, their use is limited.[3] Consequently, the discovery of new drugs that are safe, well-utilized, and effective in the treatment of UC is critical.

Intestinal barrier dysfunction is central to the pathogenesis of UC. Mucin MUC2 secreted by goblet cells is significantly reduced in UC patients, making the mucus layer thinner and leading to pathogen and antigen translocation.[4] At the same time, the expression of intestinal epithelial tight junction proteins (such as ZO-1, Occludin and Claudin4) is down-regulated, resulting in an abnormal increase in permeability.[5] In addition, the translocated pathogenic molecules activate immune cells in turn, prompting the massive release of pro-inflammatory factors such as IL-6 and TNF-α, exacerbating intestinal barrier damage.[6] Therefore, the focus of UC treatment is to achieve repair of the intestinal barrier.[7]

Intestinal stem cells (ISCs) represent an important type of adult stem cells that facilitate the daily renewal of intestinal epithelium via ongoing self-renewal, proliferation, and differentiation.[8] When injury occurs in the intestine, ISCs supplement the damaged epithelial cells and produce specific kinds of cells, such as secretory goblet cells and Paneth cells, to maintain the intestinal mucus layer integrity. This process is the core link in the repair of damaged intestinal epithelium in UC.[9] The gut microbiota and metabolites, as important components of the ISCs microenvironment, have a prospective impact on the ISCs' self-renewal function.[10]

Classic traditional Chinese medicine (TCM) formulas made from various herbs have provided medical assistance to UC patients and are often used as alternative treatment strategies.[11] Qingchang Huashi Jianpi Bushen (QCHS_JPBS) formula (Patent number: ZL201510151805.0) is derived from the Qingchang Huashi formula, which has been clinically used to alleviate the symptoms in UC patients.[12] QCHS_JPBS formula is composed of 9 Chinese medicine: *Astragalus mongholicus* Bunge (Chinese name Huangqi), *Cullen corylifolium* (L). Medik. (Chinese name Buguzhi), *Atractylodes macrocephala* Koidz. (Chinese name Baizhu), *Alpinia oxyphylla* Miq. (Chinese name Yizhiren), *Scutellaria baicalensis* Georgi (Chinese name Huangqin), *Coptis chinensis* Franch. (Chinese name Huanglian), *Aucklandia lappa* DC. (Chinese name Muxiang), *Sanguisorba officinalis* L. (Chinese name Diyu), and *Glycyrrhiza glabra* L. (Chinese name Gancao). Furthermore, our previous study demonstrated that the QCHS_JPBS formula ameliorated inflammation response in dextran sulfate sodium (DSS)-induced colitis mice.[13] Nevertheless, the potential molecular mechanisms of the QCHS_JPBS formula in treating UC need to be explained urgently.

Despite the multi-target effects, low side effects, and high efficacy of TCM, the components in TCM prescriptions are extraordinarily complex, which makes it difficult to elucidate the molecular mechanisms underlying TCM prescriptions.[14] Notably, network pharmacology is a prospective approach for revealing the active ingredients, targets, and even drug-target-disease relationships of drugs used in TCM.[15] Network pharmacological approaches have been widely used in the treatment of UC with Chinese medicines.[16] This approach provides new macroscopic insights into the treatment of UC with complex herbal medicines and offers scientific and technical support for clinical applications. In addition, an integrated strategy based on network pharmacology and experimental validation may significantly facilitate the discovery and development of anti-UC drugs.[17]

In this study, integration of multi-omics and network pharmacology analysis were applied to investigate the active components and potential molecular mechanisms of the QCHS_JPBS formula for the therapeutic amelioration of DSS-induced colitis. The results showed QCHS_JPBS formula promoted the differentiation of ISCs through gut microbiota to repair the intestinal epithelial barrier in UC mice, and potential targets for therapeutic UC with the QCHS_JPBS formulation involved EGFR, STAT3, SRC, AKT1, and HSP90AA1.

Materials and Methods

Preparation and Component Analysis of QCHS_JPBS Formula

QCHS_JPBS formula is composed of nine crude medicinal plants, *Astragalus mongholicus* Bunge (Chinese name Huangqi, 15 g), *Cullen corylifolium* (L). Medik. (Chinese name Buguzhi, 15 g), *Atractylodes macrocephala* Koidz. (Chinese name Baizhu, 10 g), *Alpinia oxyphylla* Miq. (Chinese name Yizhiren, 15 g), *Scutellaria baicalensis* Georgi (Chinese name Huangqin, 10 g), *Coptis chinensis* Franch. (Chinese name Huanglian, 3 g), *Aucklandia lappa* DC. (Chinese name Muxiang, 6 g), *Sanguisorba officinalis* L. (Chinese name Diyu, 10 g), *Glycyrrhiza glabra* L. (Chinese name Gancao, 3 g). All herbal medicines were purchased from the Jiangsu Provincial Hospital of Traditional Chinese

Medicine (Jiangsu, China). The quality of the drugs is controllable. The plant name has been verified with MPNS (http://mpns.kew.org). The herbal formula (total weight: 87 g) was soaked in 870 mL of purified water for 1 h, followed by decoction at 100°C for 40 min. The liquid was collected, and the process was repeated with an additional 870 mL of purified water under identical conditions. The liquids from the two collections were combined and concentrated to 66 mL (storage solution concentration of 1.32 g/mL) using a rotary evaporator (60 °C, 70 rpm) and stored at 4 °C.

The compositions of QCHS_JPBS formula were characterized using high-performance liquid chromatography (HPLC). An ACQUITY UPLC® HSS T3 (2.1 mm × 100 mm, 1.8 mm) was used for chromatographic separation. The flow rate and injection volume were set at 0.3 mL/min and 2 μL, respectively. For LC-ESI (+)-MS analysis, the mobile phases consisted of (B2) 0.1% formic acid in acetonitrile (v/v) and (A2) 0.1% formic acid in water (v/v). Separation was conducted under the following gradient: 0~1 min, 8% B2; 1~8 min, 8%~98% B2; 8~10 min, 98% B2; 10~10.1 min, 98% ~8% B2; 10.1~12 min, 8% B2. For LC-ESI (-)-MS analysis, the analytes were carried out with (B3) acetonitrile and (A3) ammonium formate (5mM). Separation was conducted under the following gradient: 0~1 min, 8% B3; 1~8 min, 8% ~98% B3, 8~10 min, 98% B3; 10~10.1 min, 98%~8% B3, 10.1~12 min, 8% B3. Both positive and negative-modes were applied during electrospray ionization (ESI). The ESI source conditions were as follows: Spray voltage: 3.8 kV (+) and 3.2 kV (−); Sheath Gas: 30±; Aux Gas: 5(±); Probe Heater Temp: 350 (±); S-lens RF level: 50. QCHS_JPBS formula constituents were identified by matching peak information found in Suzhou PANOMIX Co, Ltd' s in-house secondary mass spectrometry database.

Mice

SPF grade male C57BL/6 mice aged 6–8 weeks (weighting 18–22 g) were purchased from Beijing SiPeiFu Biotechnology Co., Ltd (Beijing, China). All animal procedures and experiments were assessed and approved by the Animal Ethics Committee of Nanjing University of Chinese Medicine (Approval NO. 2023DW-029-01) in accordance with the US National Institute of Health Guide for Care and Use of Laboratory Animals.

Establishment and Drug Administration of Colitis in Mice

Mice were exposed to 2.5% DSS (Cat # 160110, MP Biomedicals, USA) in drinking water for 7 days and then treated with normal drinking water for 7 days to establish colitis. Mice were randomized into five groups (n=6): normal, model, low-dose QCHS_JPBS formula, high-dose QCHS_JPBS formula, and 5-ASA. According to the dose used in clinical patients (87 g/60 kg), mice were given QCHS_JPBS at a dose of 7.6 g/kg or 13.2 g/kg, and the dose of 5-ASA (Cat # 79809, Sigma-Aldrich, USA) was 100 mg/kg. From days 8–14, different concentrations of the drug were given by gavage in the drug group, while the normal and Model groups were given the same volume of the solvent.

Histological and Immunohistochemical Analyses

Colon tissues from mice were collected and fixed with 4% formaldehyde. Then, the colon tissues were embedded in paraffin and processed for histological analysis. The fixed colon tissues were sliced into 5 μm size sections and stained with H&E, PAS, AB/PAS.

Quantitative Real-Time PCR

Total RNA was extracted from colon tissues using TRIzol extraction reagent (Cat # 15596026, Invitrogen, USA) according to the manufacturer's instructions. The cDNA was reverse transcribed using a Hifair@ III 1st Stand cDNA Synthesis Super Mix (Cat #Q71102, Vazyme, China). RT-qPCR analysis was carried out using Hieff@ qPCR SYBR green master mix (Cat # R32301, Vazyme, China) on a Roche Light Cycler 96 system. The primers used are listed in Table 1.

Western Blot Assay

Total protein was extracted from colon tissue using RIPA buffer containing 1% PMSF. Proteins were then separated by 10–12% SDS-PAGE, transferred to polyvinylidene difluoride membranes, blocked with 5% skimmed milk in TBST for

Table 1 Primers Used for Quantitative Real-Time PCR

Gene	Primer Sequences (5'-3')	
	Forward	Reverse
Tnf-α	AAGGCCGGGGTGTCCTGGAG	AGGCCAGGTGGGGACAGCTC
Il-6	CCACTTCACAAGTCGGAGGCTTA	AGTGCATCATCGTTGTTCATAC
Il-1β	GAATGCCACCTTTTGACAGTG	TGGATGCTCTCATCAGGACAG
Il-10	CTTACTGACTGGCATGAGGATCA	GCAGCTCTAGGAGCATGTGG
Zo-1	GTCCCTGTGAGTCCTTCAGC	TAGGGTCACAGTGTGGCAAG
Claudin-4	ACGTCATCCGCGACTTCTAC	TTGTCGTTGCTACGAGGTGG
Lgr5	CCTACTCGAAGACTTACCCAGT	GCATTGGGGTGAATGATAGCA
Msi-1	TCGGAGGACTCAGTTGGCAGAC	CCCGCATCACCAGACACTCTTTC
Olfm4	CAGCCACTTTCCAATTTCACTG	GCTGGACATACTCCTTCACCTTA
Lysozyme	GAGCTGTGAATGCCTGTGGGATC	GACAGTGTGCTCGCCATGCC
Chromogranin A	CAGAGACGCAGCAGCAGAAGTG	AAAGCCATCCTGTTGTCCCTTGTC
β-actin	CTCATGAAGATCCTGACCGAG	AGTCTAGAGCAACATAGCACAG

1 h at room temperature. The membranes were incubated with specific primary antibodies (1:1000, ZO-1 (Cat # 33735, Santa Cruz Biotechnology, USA), Claudin-4 (Cat # 53156, Abcam, USA), LGR5 (Cat # BM4244, BOSTER, China), Msi-1 (Cat # A05052-1 BOSTER, China), Lysozyme (Cat # PB9663, BOSTER, China), Chromogranin A (Cat # bs-43559R, BIOSYNTHESIS, China), Actin (Cat # 66009, Proteintech, China)) against the membrane overnight at 4°C and appropriate secondary antibodies (1:5000, HRP conjugated goat anti-mouse (Cat # 15014, Proteintech, China), HRP conjugated goat anti-rabbit (Cat # 15015, Proteintech, China)) against the membrane at room temperature for 2 h. The bands were visualized with an enhanced chemiluminescent reagent using the ChemiDocTM XRS + system (Bio-rad, Hercules, CA, USA). A picture of the blot marker used in this experiment was shown in Figure 1 of the Supplementary Material, and the raw data of Western blot were shown in Figures 2–5 of the Supplementary Material, respectively.

16S rRNA Sequencing of Cecal Contents

Colon fecal contents were snap frozen with liquid nitrogen and stored at −80 °C. Genomic DNA was extracted from fecal samples using PF Mag-Bind Stool DNA Kit (Omega Bio-tek, Georgia, US) according to the manufacturer's protocols. The hypervariable region V3-V4 of the bacterial 16S rRNA gene were amplified with primer pairs 515F (5'-GTGCCAGCMGCCGCGG-3') and 907R (5'- CCGTCAATTCMTTTRAGTTT-3') by an ABI GeneAmp® 9700 PCR thermocycler (ABI, CA, USA). The PCR product was extracted from 2% agarose gel and purified. Then quantified using Quantus™ Fluorometer (Promega, USA). Purified amplicons were pooled in equimolar amounts and paired-end sequenced on an Illumina PE250 platform (Illumina, San Diego,USA) according to the standard protocols by Majorbio Bio-Pharm Technology Co. Ltd. (Shanghai, China). Raw FASTQ files were de-multiplexed using an in-house perl script, and then quality-filtered by fastp version 0.19.6 and merged by FLASH version 1.2.11. Then the optimized sequences were clustered into operational taxonomic units (OTUs) using UPARSE 11 with 97% sequence similarity level. Bioinformatic analysis of the gut microbiota was carried out using the Majorbio Cloud platform (https://cloud.majorbio.com).

Metabolome Analysis of Cecal Contents

A total of 50 mg sample was added to a 2 mL centrifuge tube and a 6 mm diameter grinding bead was added. A total of 400 μL of extraction solution (methanol: water = 4:1 (v:v)) containing 0.02 mg/mL of internal standard (L-2-chlorophenylalanine) was used for metabolite extraction. Samples were ground by the Wonbio-96c (Shanghai wanbo biotechnology co., LTD) frozen tissue grinder for 6 min (−10 °C, 50 hz), followed by low-temperature ultrasonic extraction for 30 min (5 °C, 40 kHz). The samples were left at −20 °C for 30 min, centrifuged for 15 min (4 °C, 13000 g), and the supernatant was transferred to the injection vial for LC-MS/MS analysis.

The intracellular metabolic profile was conducted on a Thermo UHPLC-Q Exactive HF-X system equipped with an ACQUITY HSS T3 column (100 mm × 2.1 mm i.d., 1.8 μm; Waters, USA) at Majorbio Bio-Pharm Technology Co. Ltd.

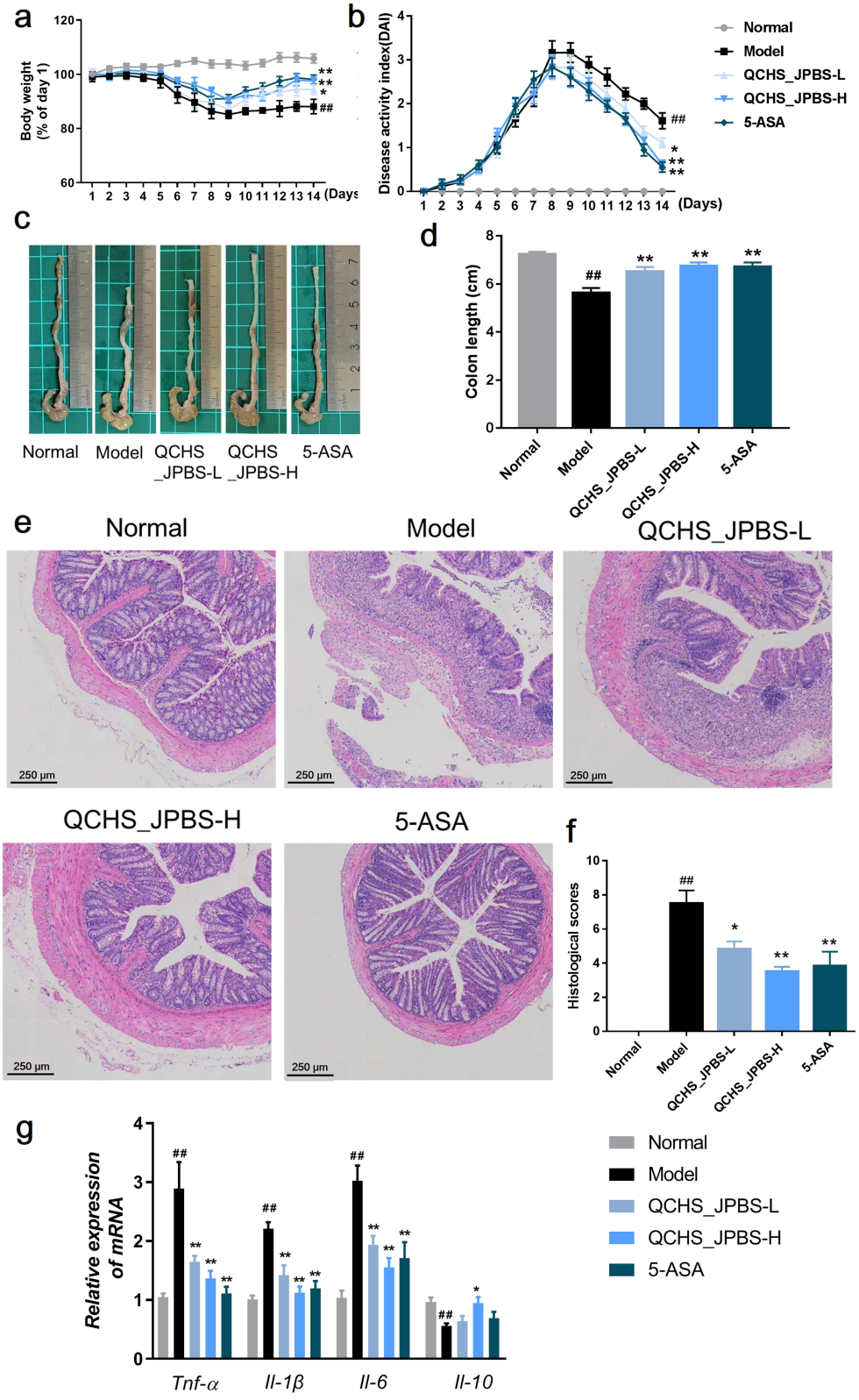

Figure 1 QCHS_JPBS formula promotes recovery of DSS-induced colitis in mice. Colitis was induced in mice by drinking with 2.5% DSS for 7 days. QCHS_JPBS formula (6.6, 13.2 g/kg) was orally administered for consecutive 7 days. 5-ASA (100 mg/kg) was used as a positive control. (**a**) Percent body weight change. (**b**) DAI evaluation. (**c** and **d**) Colon length. (**e** and **f**) H&E staining and pathologic scoring of colon tissue. (**g**) The expression level of inflammation-related factors in colon tissue. Data are expressed as the means ± S.E.M., $^{\#\#}P < 0.01$ versus Normal, $^{*}P < 0.05$ and $^{**}P < 0.01$ versus Model.

https://doi.org/10.2147/JIR.S510966

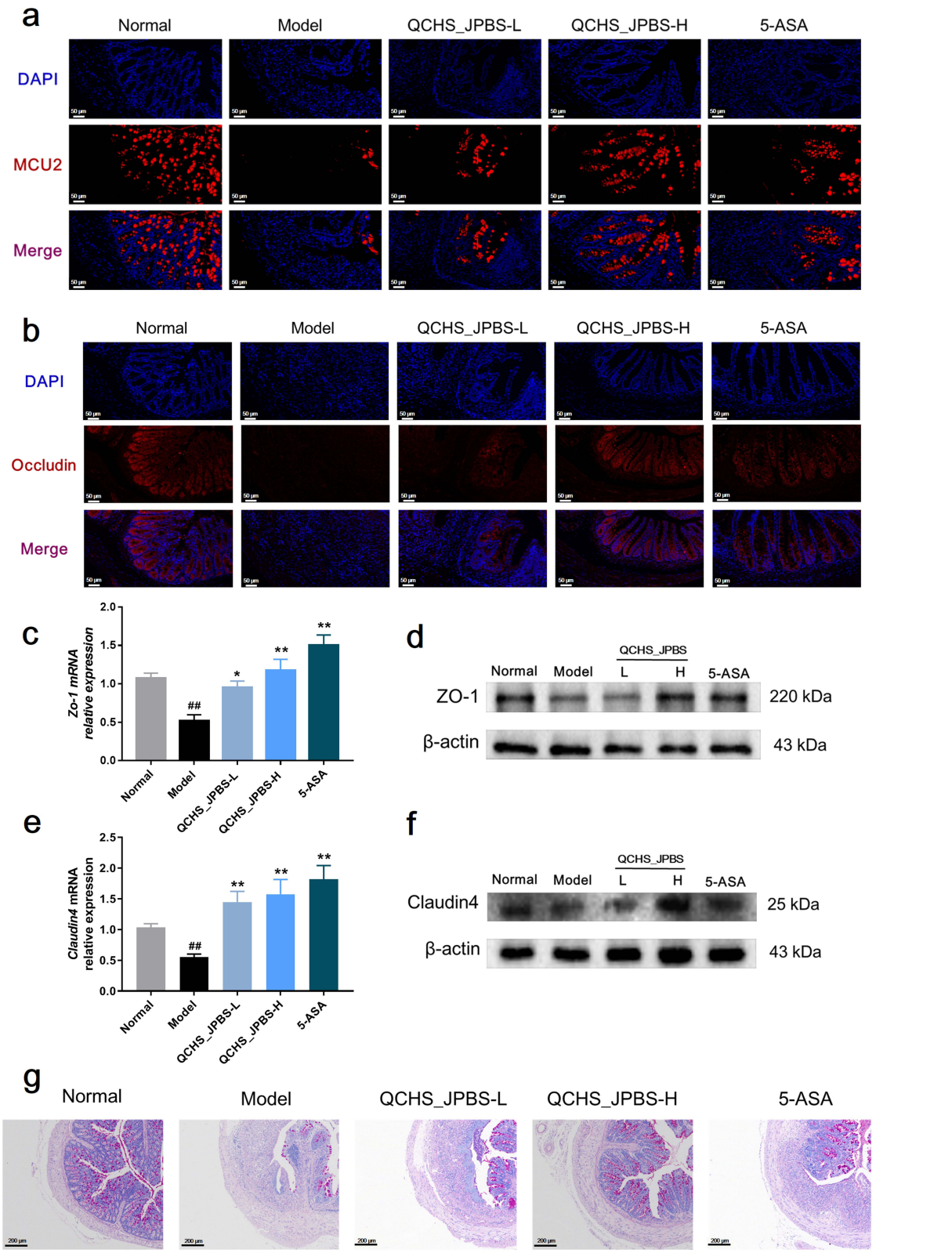

Figure 2 QCHS_JPBS formula repairs the intestinal epithelial barrier in DSS-induced colitis mice. (**a** and **b**) Immunofluorescence staining for MUC2 and Occludin in colon tissue. (**c** and **d**) The expression levels of ZO-1 mRNA and protein in colon tissue. (**e** and **f**) The expression levels of Claudin4 mRNA and protein in colon tissue. (**g**) PAS staining of colon tissue. Data are expressed as the means ± S.E.M., $^{\#\#}P < 0.01$ versus Normal, $^{*}P < 0.05$ and $^{**}P < 0.01$ versus Model.

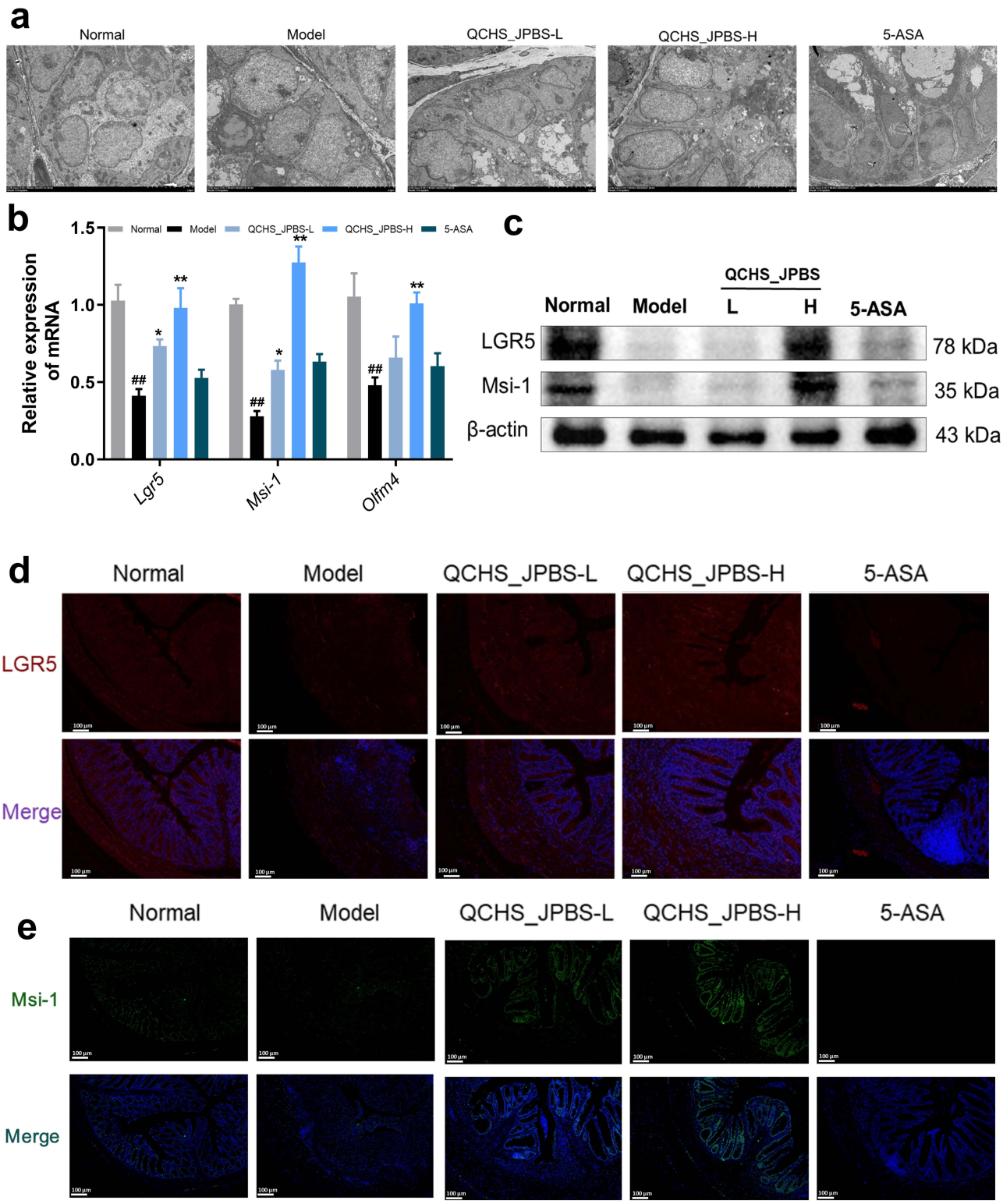

Figure 3 QCHS_JPBS formula promotes ISCs differentiation in DSS induced-colitis mice. (**a**) Colonic crypt structure. (**b**) The expression levels of LGR5, Msi-1 and Olfm4 mRNA in colon tissue. (**c**) The expression levels of LGR5 and Msi-1 protein in colon tissue. (**d** and **e**) Immunofluorescence staining for LGR5 and Msi-1 in colon tissue. Data are expressed as the means ± S.E.M., $^{\#\#}P < 0.01$ versus Normal, $^{*}P < 0.05$ and $^{**}P < 0.01$ versus Model.

https://doi.org/10.2147/JIR.S510966

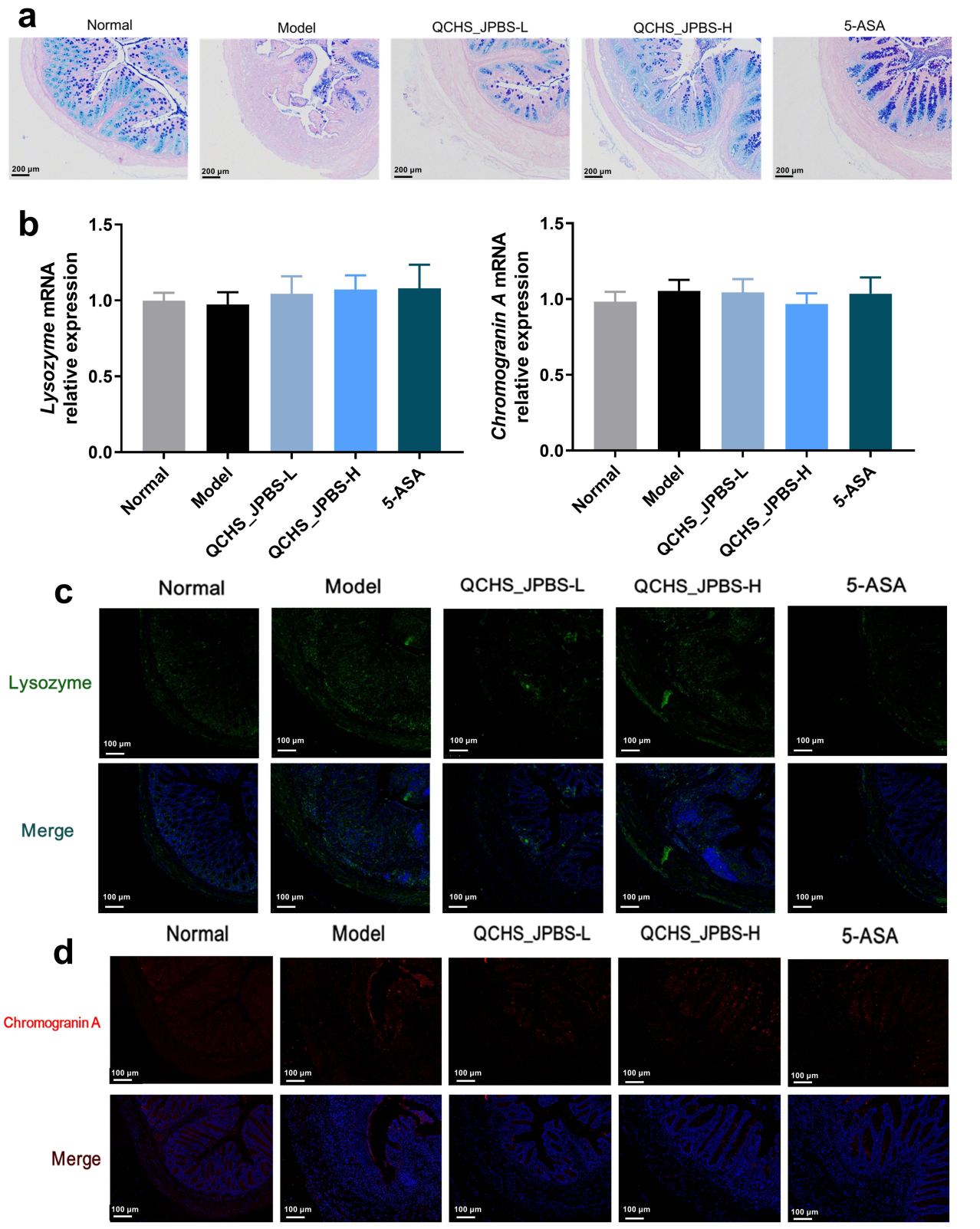

Figure 4 QCHS_JPBS formula promotes the differentiation of ISCs into goblet cells. (**a**) AB-PAS staining of colon tissue. (**b**) The expression levels of Lysozyme and Chromogranin A mRNA in colon tissue. (**c** and **d**) Immunofluorescence staining for Lysozyme and Chromogranin A in colon tissue. Data are expressed as the means ± S.E.M.

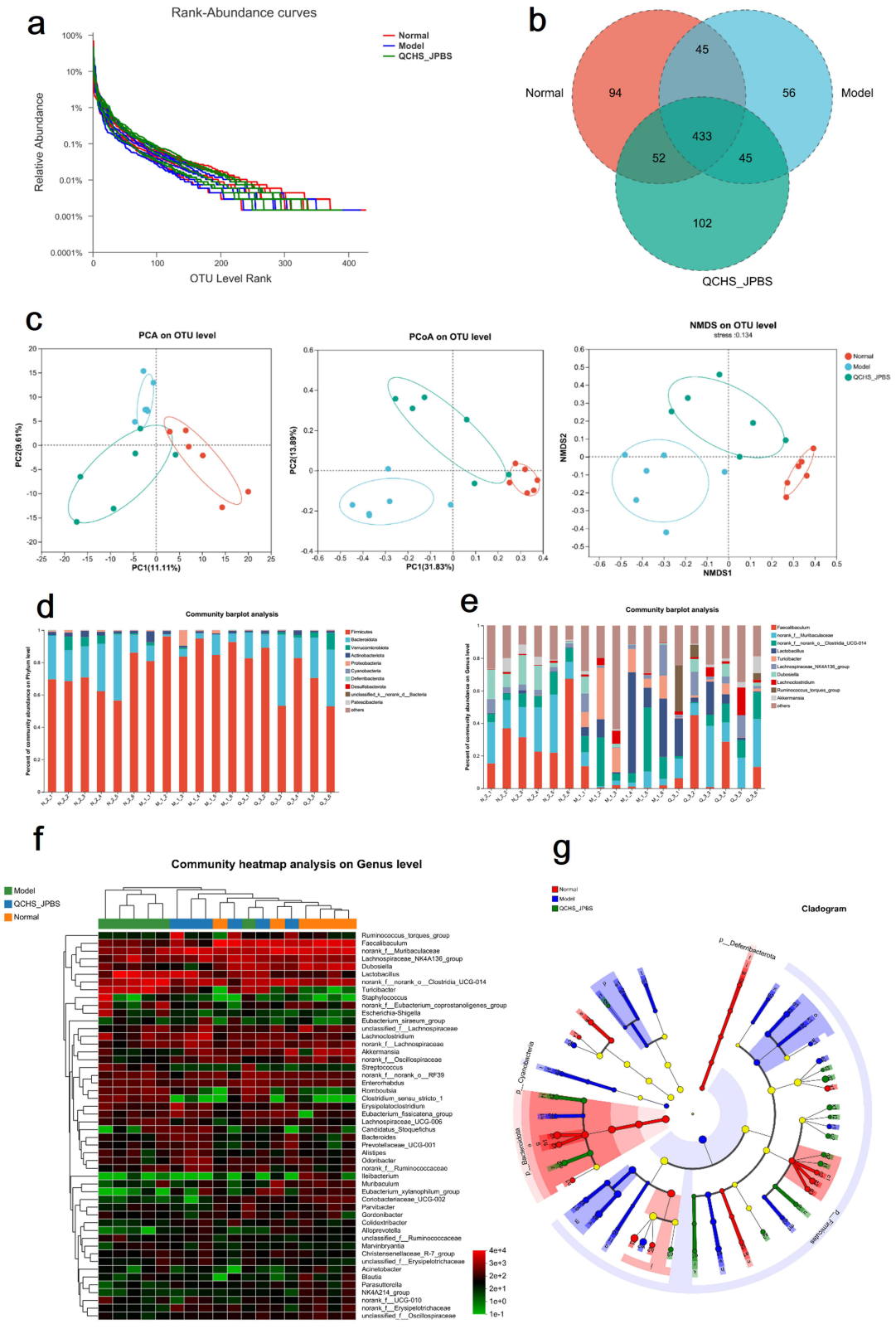

Figure 5 QCHS_JPBS formula restores gut dysbiosis in DSS-induced colitis mice. Collect mouse cecal contents for 16S rRNA analysis. (**a**) The relative abundance of each OTU and OTU rank curve. (**b**) The overlap of OTUs across groups was presented using a Venn diagram. (**c**) Principal component analysis (PCA) showed significant differences in gut microbiota β diversity. (**d** and **e**) The relative bacterial abundance at the phylum and genus levels was shown. (**f**) The relative abundance of bacteria in genus level and heatmap clustering analysis. (**g**) LEfSe analysis and the taxonomic cladogram.

https://doi.org/10.2147/JIR.S510966

(Shanghai, China). The mobile phases consisted of 0.1% formic acid in water: acetonitrile (95:5, v/v) (solvent A) and 0.1% formic acid in acetonitrile: isopropanol: water (47.5:47.5:5, v/v) (solvent B). The flow rate was 0.40 mL/min and the column temperature was 40 °C. The injection volume was 3 μL.

The mass spectrometric data were collected using a Thermo UHPLC-Q Exactive HF-X Mass Spectrometer equipped with an electrospray ionization (ESI) source. The scan range was from 100–1000 m/z for positive and negative ion mode. The detailed parameters were as follows: sheath gas temperature, 325 °C; capillary voltage of 3500 V (+) and 3500 V (-). The pretreatment of LC/MS raw data was performed by Progenesis QI (Waters Corporation, Milford, USA) software. The data matrix obtained by searching database was uploaded to the Majorbio cloud platform (https://cloud.majorbio.com) for data analysis.

Fecal Microbiota Transplantation

The procedure of fecal microbial transplantation (FMT) was carried out in accordance with the previous study.[18,19] Ten donor mice were randomly divided into two groups including Control group and QCHS_JPBS group (n=5). Collect feces from mice treated with the QCHS_JPBS formula for 14 days or from control mice. A total of 100 mg of feces were resuspended in 1 mL of sterile saline solution. The solution was vigorously mixed for 15s, then centrifuged at 800×g for 5 min and the supernatant was collected. Fresh transplant material was prepared within 10 min prior to oral administration on the day of transplantation to avoid changes in bacterial composition.

The recipient mice were fed with antibiotic water (500 μg/mL ampicillin, 500 μg/mL metronidazole, 250 μg/mL vancomycin, and 500 μg/mL neomycin) for 10 days to clear the gut microbiota. Recipient mice were randomly assigned into three groups (n=6): Control→Control group, Control→DSS group, QCHS_JPBS→DSS+QCHS_JPBS group. Each group of mice was given transplant material for 10 consecutive days. On the 4th day, 2.5% DSS (w/v) was administered to induce enteritis for 7 consecutive days. Subsequently, the mice were euthanized and colon tissue was collected.

Network Pharmacology Analysis

The mechanism of QCHS_JPBS formula in relieving UC was further explored using network pharmacological analysis. The TCMSP database (https://www.tcmsp-e.com/) was used to MOL-ID tag the identified components. The disease targets of the components were predicted (http://www.swisstargetprediction.ch/). The UC therapeutic targets were retrieved from the OMIM database (https://omim.org/), Genecards database (https://www.genecards.org), TTD database (https://db.idrblab.net/ttd/), and Drugbank database (https://go.drugbank.com). Target names were converted to gene symbols using the UniProKB database (https://www.uniprot.org) and subsequently input into the STRING database (https://string-db.org) for protein-protein interaction (PPI) analysis. The interaction networks were visualized using Cytoscape software (https://www.cytoscape.org/). Gene Ontology (GO) enrichment and Kyoto Encyclopedia of Genes and Genomes (KEGG) pathway enrichment analysis were conducted using the Metascape databases (https://metascape.org/). The results were imported and visualized on a bioinformatics platform (https://www.bioinformatics.com.cn/).

Statistical Analysis

Statistical analyses were conducted with Prism 8 software (GraphPad Software, La Jolla, CA, USA). Data are expressed as the means ± S.E.M. One-way ANOVA was used for comparing the mean differences between multiple groups. A value of $P < 0.05$ was defined as a significant.

Results

QCHS_JPBS Formula Promotes Recovery of DSS-Induced Colitis in Mice

To investigate the therapeutic effect of QCHS_JPBS formula in UC, DSS-induced colitis mice were treated with QCHS_JPBS formula, with 5-ASA as a positive control. The body weight of mice recovered after treatment with QCHS_JPBS formula or 5-ASA compared to their starting weight (Figure 1a), meanwhile the DAI score was dropped after QCHS_JPBS formula or 5-ASA treatment (Figure 1b). In addition, there was a significant lengthening trend of colon after QCHS_JPBS formula treatment (Figure 1c and d). The results of H&E staining revealed that QCHS_JPBS

formula or 5-ASA restored the DSS-induced damage in colon villous morphology and crypt. The QCHS_JPBS formula treatment groups obviously alleviated the pathological condition (Figure 1e and f). QCHS_JPBS formula could also reduce the expression level of inflammatory factors and promote the expression level of anti-inflammatory factors in intestinal tissue (Figure 1g). Altogether, these results demonstrated that QCHS_JPBS formula therapy improved the symptoms of UC mice.

QCHS_JPBS Formula Repairs the Intestinal Epithelial Barrier in DSS-Induced Colitis Mice

Since UC can result in direct damage to the intestinal epithelial barrier, the healing of the mucosa has emerged as the latest goal in UC treatment. Therefore, whether the QCHS_JPBS formula could repair the damaged intestinal epithelial barrier in UC mice has been investigated. The results of immunofluorescence showed that QCHS_JPBS formula treatment could significantly promote the expression of MUC2 and Occludin proteins, thereby reducing intestinal mucosal damage (Figure 2a and b). ZO-1 and Claudin4 were improved after treatment with QCHS_JPBS formula at both mRNA and protein levels (Figure 2c–f). In addition, The PAS staining evaluation results showed that QCHS_JPBS formula treatment could increase mucoprotein secretion (Figure 2g). These results implied that the administration of QCHS_JPBS formula could significantly augment the mucosal integrity in DSS-induced colitis.

QCHS_JPBS Formula Promotes ISC Differentiation in DSS Induced-Colitis Mice

Research shows that the differentiation of ISCs is a core link in the repair of UC-damaged intestinal epithelium. Therefore, whether QCHS_JPBS formula has an impact on the differentiation of ISCs will be further investigated. The structure of the colon crypt was observed using transmission electron microscopy, and the results revealed that the integrity of the colon crypt structure in mice treated with QCHS_JPBS formula was higher compared with the model group (Figure 3a). The results showed that compared with the DSS group, the mRNA expression levels of ISC differentiation markers, such as LGR5, Msi-1 and Olfm4, were elevated in colon tissues after intervention with QCHS_JPBS formula (Figure 3b). In addition, Western blotting and immunofluorescence assays also showed that the protein expression levels of LGR5 and Mis-1 were significantly increased after the intervention of QCHS_JPBS formula (Figure 3c–e). These results indicated that QCHS_JPBS formula could promote the differentiation of ISCs.

What's more, research was conducted on the subtypes of ISC differentiation promoted by QCHS_JPBS formula. The results revealed that the number of colon goblet cells labeled with AB-PAS staining increased after the intervention of QCHS_JPBS formula compared with the model group (Figure 4a). Subsequently, the effect of the QCHS_JPBS formulation intervention on the differentiation of Paneth cells and endocrine cells was assessed using RT-qPCR assays. The results of this study showed that the QCHS_JPBS formulation had no significant effect on the expression of two cell-specific markers, Lysozyme and Chromogranin A, respectively, compared to the model group (Figure 4b). Furthermore, colon tissue immunofluorescence demonstrated similar results (Figure 4c and d). In summary, these results suggested that the subtype of ISCs differentiation mainly controlled by QCHS_JPBS formula was goblet cells.

QCHS_JPBS Formula Restores Gut Dysbiosis in DSS-Induced Colitis Mice

As the commensal microbiota in the intestine has a key role in sustaining intestinal balance, and dysbiosis of the intestinal microbiota has been shown to be closely associated with the onset and progression of colitis. Therefore, 16S rRNA sequencing was used to detect the structural changes in the gut microbiota of UC mice after the intervention of QCHS_JPBS formula. The results showed differences in the number and structure of OTUs in the gut microbiota of mice between groups (Figure 5a and b). Principal component analysis (PCA) showed significant differences in gut microbiota β diversity among the normal group, model group, and QCHS_JPBS formula group mice. The above results suggested that the intervention of QCHS_JPBS formula could alter the intestinal microbiota structure of UC model mice (Figure 5c). Subsequently, the differences in the relative abundance of gut microbiota among the three groups were analyzed. At the phylum level, the abundance of *Firmicutes* increased, while the abundance of *Bacteroidetes* decreased in the feces of DSS-induced colitis mice, and the intervention of QCHS_JPBS formula could reverse this change (Figure 5d). At the genus level, the relative

 https://doi.org/10.2147/JIR.S510966

abundance of *Clostridia* and *Lactobacillus* increased, while the relative abundance of *Faecalibaculum* and *Muribaculaceae* decreased in the feces of DSS induced colitis mice, and the intervention of QCHS_JPBS formula could reverse this change (Figure 5e). Heat-map analysis and linear discriminant analysis effect size (LEfSe) analysis indicated that after QCHS_JPBS formula treatment, the abundance of dominant bacteria shown an upward trend (Figure 5f and g). These results illustrated that QCHS_JPBS formula could modulate the gut microbiota to attain a new homeostasis by restoring the abundance of dominant bacteria.

QCHS_JPBS Formula Regulates Metabolic Disorders in DSS-Induced Colitis Mice

Metabolites are important mediators for the gut microbiota to exert effects. Therefore, untargeted metabolomics was conducted to investigate the effect of QCHS_JPBS formula on the fecal metabolomics of DSS-induced colitis mice. The metabolic changes in the three groups of mice were investigated using principal component analysis (PCA). The results showed significant differences in the metabolic structure of feces among the three groups of mice (Figure 6a). In addition, OPLS-DA showed metabolites that potentially contributed to the classification of the samples (Figure 6b). The Venn diagram visually displays the common and unique differential metabolites between each group (Figure 6c). The overall differences metabolites between the QCHS_JPBS formula groups and model groups were demonstrated using volcano and heat maps (Figure 6d and e). Pathway analysis of differential metabolites was conducted based on the KEGG database. The results showed that signaling pathways such as sphingolipids metabolism were enriched (Figure 6f). Together, these results provided clear evidence that DSS-induced colitis mice exhibited significant metabolic disorders in feces, and QCHS_JPBS formula could restore metabolic imbalances in UC mice.

QCHS_JPBS Formula Promotes Intestinal ISCs Through Gut Microbiota

To further clarify the positive effects of QCHS_JPBS formula mediated through the gut microbiota and its effects on intestinal inflammation response, the microbiota originating from QCHS_JPBS formula-treated mice was transferred to DSS-fed mice, and then assayed for colitis-related traits (Figure 7a). The results showed that mice receiving the QCHS_JPBS formula-treated donor microbiota recovered faster. This result was also demonstrated in body weight recovery and DAI decrease compared to DSS-treated recipients of control microbiota (Figure 7b and c). Moreover, a statistically significant trend was lengthened colon in the recipients of microbiota from QCHS_JPBS formula-treated donors compared to the control (Figure 7d and e). The H&E staining results showed a decrease in histopathological scores in the recipients of microbiota from QCHS_JPBS formula-treated donors (Figure 7f and g).

In addition, the mRNA expression levels of ISC differentiation markers, such as LGR5, Msi-1 and Olfm4, were elevated in colon tissues after the intervention with microbiota from QCHS_JPBS formula-treated donors (Figure 8a). What's more, Western blotting and immunofluorescence assays also showed that the protein expression levels of LGR5 and Mis-1 were significantly increased after the intervention with microbiota from QCHS_JPBS formula-treated donors (Figure 8b–d). Finally, AB-PAS staining showed that the number of epithelial cells was higher in mice treated with QCHS_JPBS-formulated donor microbiota (Figure 8e). These results suggest that the QCHS_JPBS formula promotes ISC integration via the gut microbiota, thereby repairing the mucosal barrier in colitis.

Analysis of Potential Anti-Colitis Mechanisms of QCHS_JPBS Formula Using Network Pharmacology

The main representative components, such as Astragaloside IV, Atractylenolide III, Isopsoralen, Chrysin, Baicalin, Berberine, Gallic acid, Costunolide, and Glycyrrhizin, were identified by comparing the retention time in QCHS_JPBS formula, which demonstrated that the major ingredients of QCHS_JPBS formula had stability and reproducibility. The chromatogram and chemical structure of the representative components involved in the QCHS_JPBS formula were depicted in Figure 9. In addition, a total of 79 active ingredients were identified and listed in Table 2.

Network pharmacology analysis was performed to elucidate the underlying mechanism of QCHS_JPBS formula anti-colitis. With "ulcerative colitis" as the key word, A total of 2983 disease targets were gained from OMIM, GeneCards, TTD and Drugbank databases. A total of 752 therapeutic target proteins associated with 79 active ingredients of

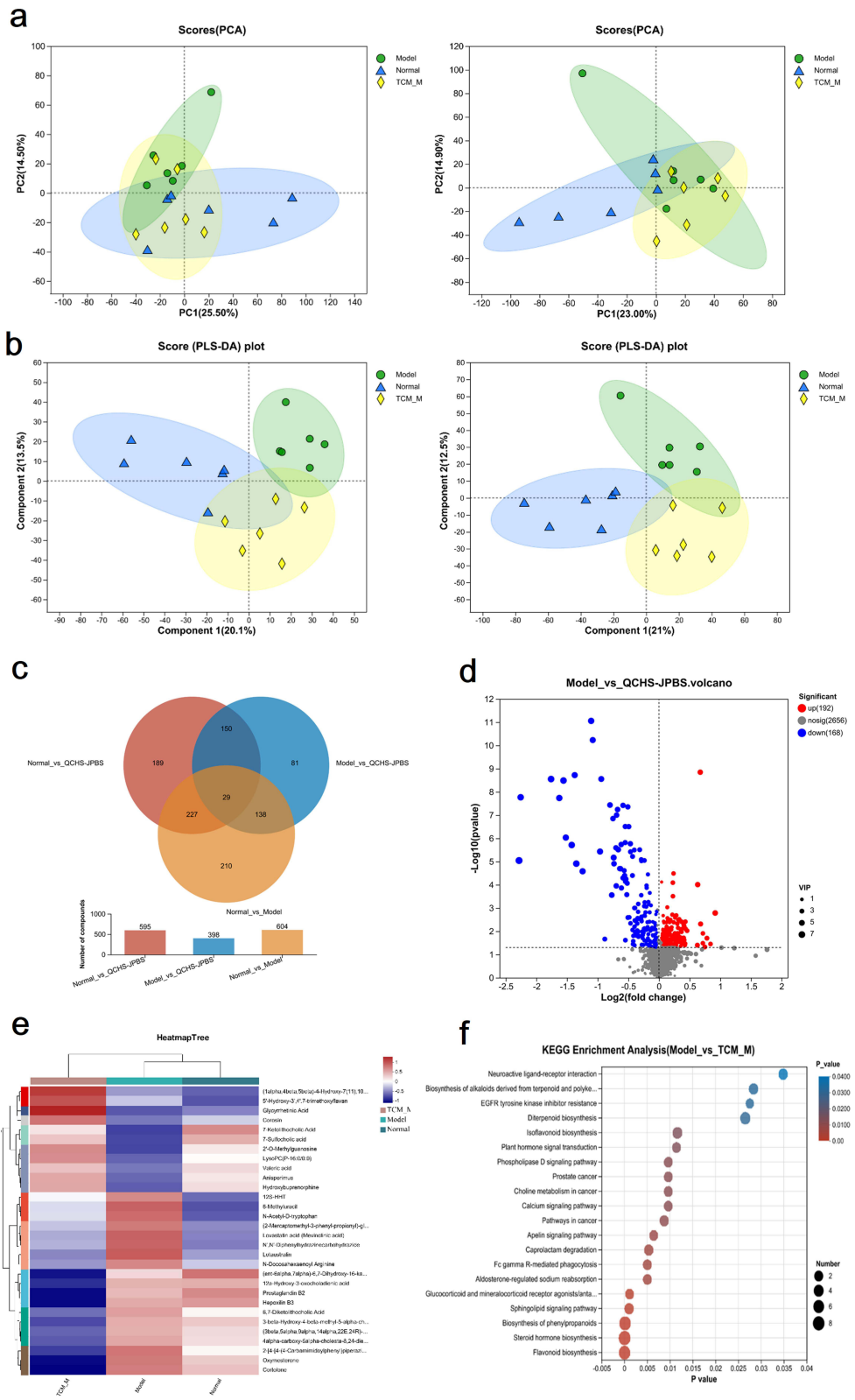

Figure 6 QCHS_JPBS formula regulates metabolic disorders in DSS-induced colitis mice. Mouse feces were subjected to non-target metabolomics analysis based on UHPLC-MS. (**a**) The PCA scores plots of samples under positive and negative ion mode. (**b**) The PLS-DA scores plot of samples under positive and negative ion modes. (**c**) The Venn diagram analysis of different metabolites among three groups. (**d**) The volcano plot shown significant changes in metabolites between QCHS_JPBS formula and the model group, with each point representing a metabolite. (**e**) The heatmap shown the changed concentrations of potential significantly differential metabolites. (**f**) A schematic diagram of metabolic pathways displayed based on differential metabolites.

https://doi.org/10.2147/JIR.S510966

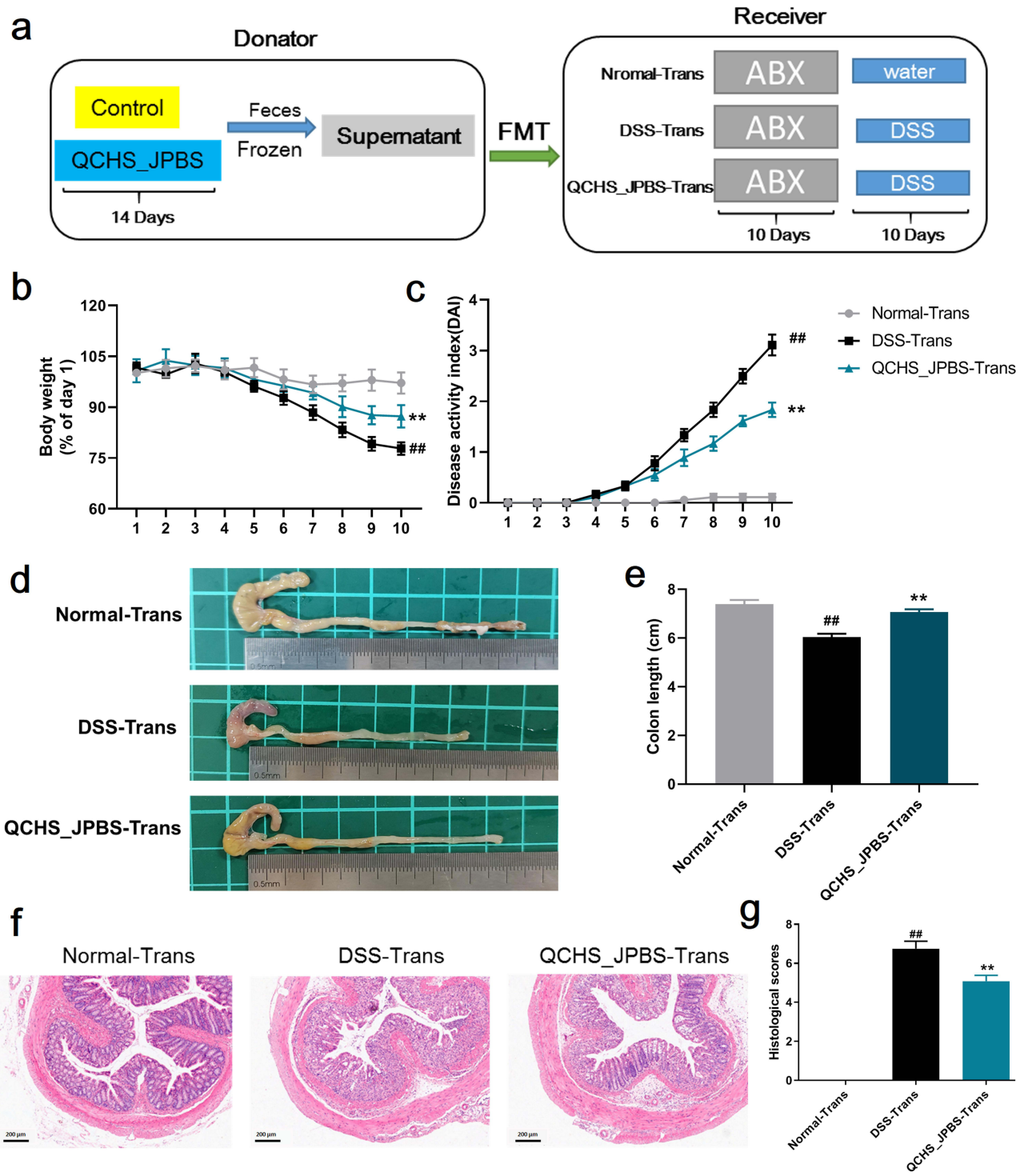

Figure 7 QCHS_JPBS formula promotes recovery of DSS-induced colitis in mice through gut microbiota. The microbiota of QCHS_JPBS formula-treated mice were transferred to DSS-fed mice, and then subjected to examination of colitis-related traits. (**a**) Diagram illustrating the mouse model of colitis employed in this study. (**b**) Percent body weight change. (**c**) DAI evaluation. (**d** and **e**) Colon length. (**f** and **g**) H&E staining and pathologic scoring of colon tissue. Data are expressed as the means ± S.E. M., $^{\#\#}P < 0.01$ versus Normal-Trans, $^{**}P < 0.01$ versus DSS-Trans.

QCHS_JPBS formula were predicted. Then, the 362 overlapping targets were retained as candidate targets (Figure 10a). To identify targets that have direct or indirect interactions, the 362 overlapping genes were imported into the STRING database and a PPI network was constructed, including 362 nodes and 7945 edges (Figure 10b). For further visualization

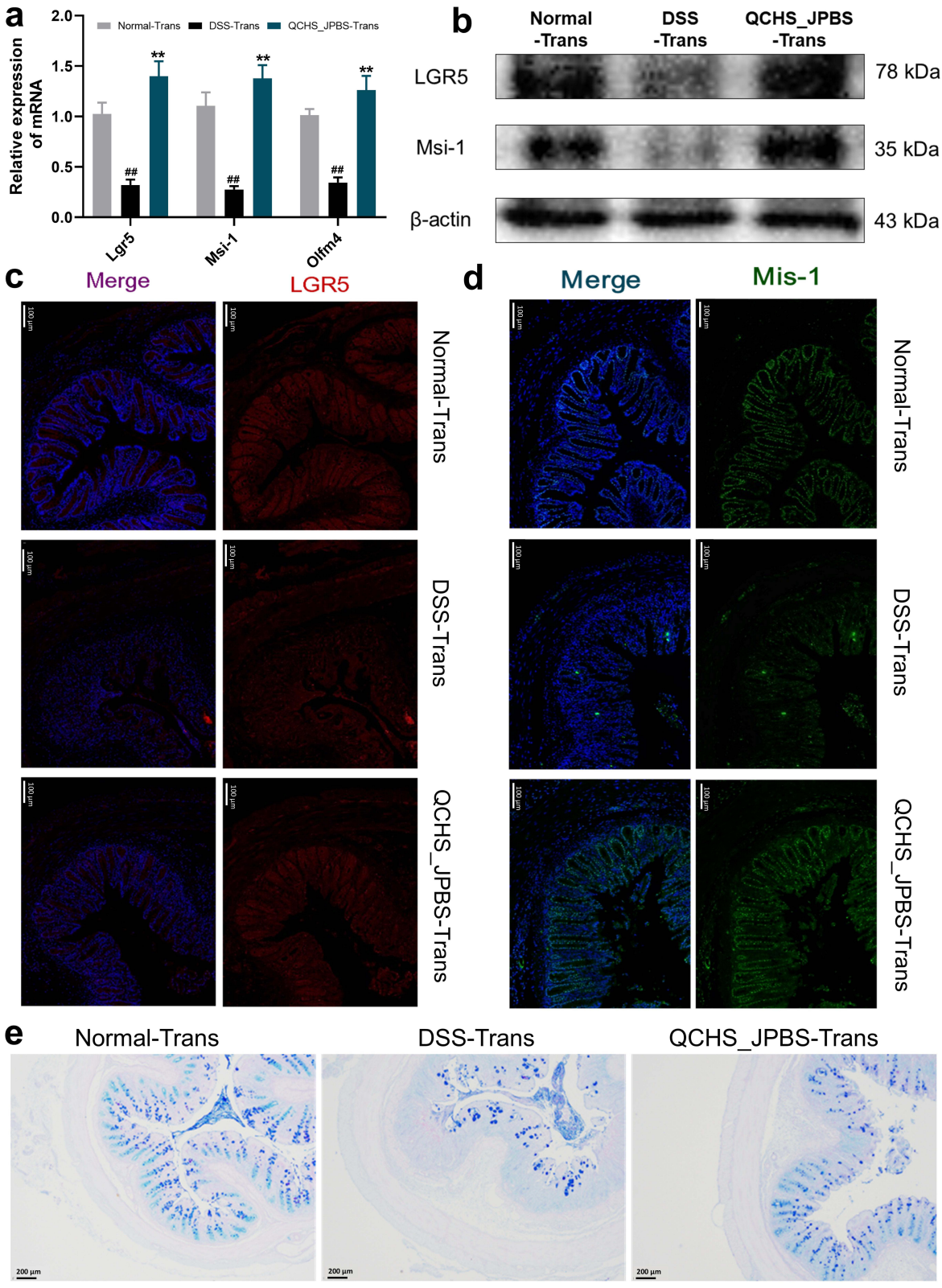

Figure 8 QCHS_JPBS formula promotes ISCs through gut microbiota. (**a**) The expression levels of LGR5, Msi-1 and Olfm4 mRNA in colon tissue. (**b**) The expression levels of LGR5 and Msi-1 protein in colon tissue. (**c** and **d**) Immunofluorescence staining for LGR5 and Msi-1 in colon tissue. (**e**) AB-PAS staining of colon tissue. Data are expressed as the means ± S.E.M., $^{\#\#}P < 0.01$ versus Normal-Trans, $^{**}P < 0.01$ versus DSS-Trans.

https://doi.org/10.2147/JIR.S510966

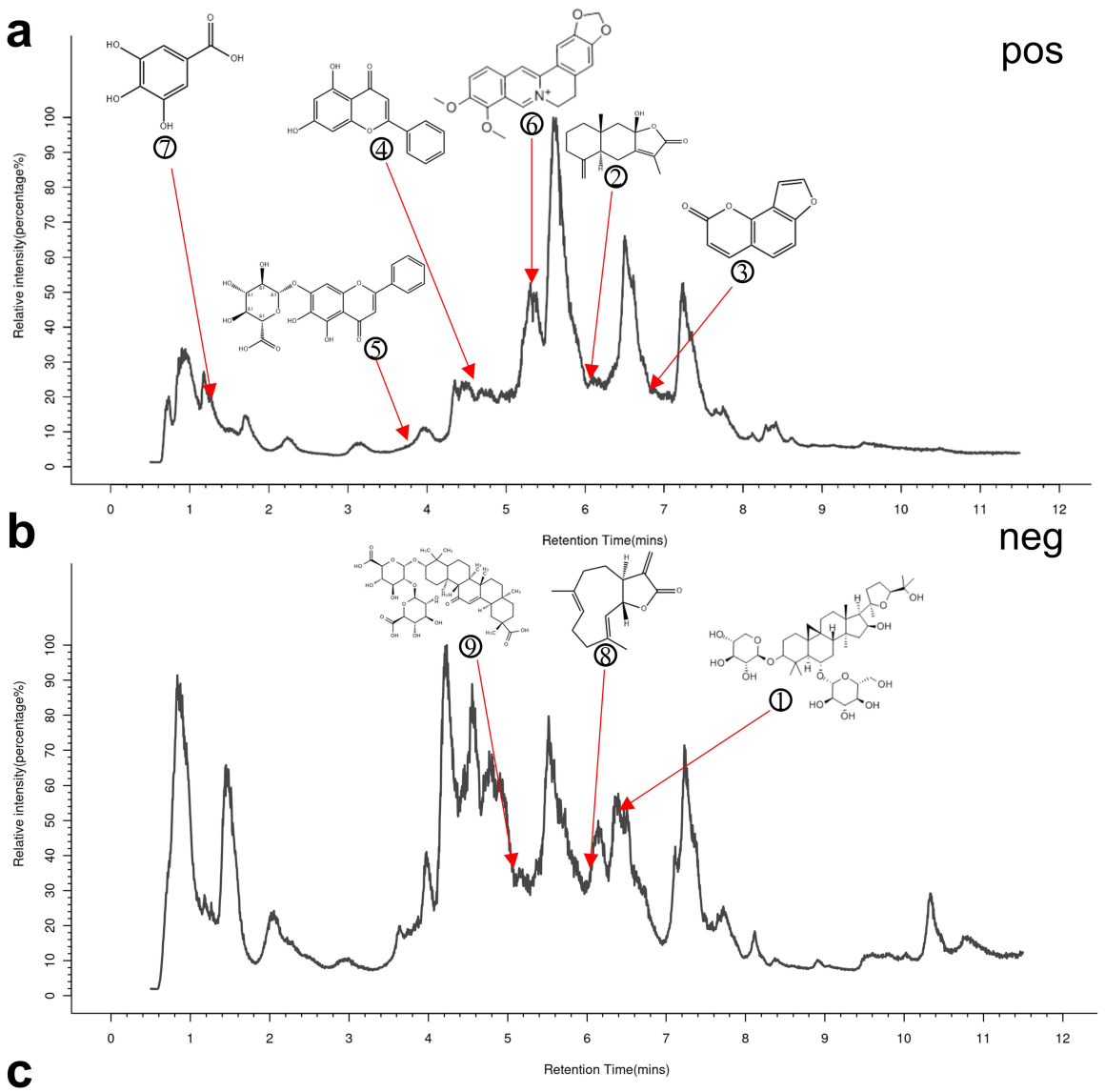

c

No.	Name	Formula	Class	RT(min)	Intensity
①	Astragaloside IV	$C_{41}H_{68}O_{14}$	Terpenoids	6.3150	19898885.61
②	Atractylenolide III	$C_{15}H_{20}O_3$	Terpenoids	5.9883	788776509.2
③	Isopsoralen	$C_{11}H_6O_3$	Phenylpropanoids	6.6100	98264223150
④	Chrysin	$C_{15}H_{10}O_4$	Flavonoids	4.6667	158026696.7
⑤	Baicalin	$C_{21}H_{18}O_{11}$	Flavonoids	3.8950	355673621.3
⑥	Berberine	$C_{20}H_{18}NO_4$	Alkaloids	5.3000	4800455169
⑦	Gallic acid	$C_7H_6O_5$	Phenylpropanoids	1.3200	105683218.3
⑧	Costunolide	$C_{15}H_{20}O_2$	Terpenoids	5.9683	776729150.2
⑨	Glycyrrhizin	$C_{42}H_{62}O_{16}$	Terpenoids	5.0050	988315071.7

Figure 9 Identification of representative ingredients in QCHS_JPBS formula using UHPLC-MS/MS. (**a**) The positive mode. (**b**) The negative mode. (**c**) The chemical structure and extracting ion chromatography (EIC) of representative compounds in QCHS_JPBS formula.

Table 2 QCHS_JPBS Formula Identified Component Information

No.	Name	RT(min)	Formula	Class	Precursor_Type	pos/neg	Intensity	MOL ID
1	Gallic acid	1.3200	C7H6O5	Phenylpropanoids	[M+H]+	pos	105683218.3	MOL000513
2	Psoralen	0.5967	C11H6O3	Phenylpropanoids	[M+H]+	pos	13854726.2	MOL001950
3	Angelicin	6.6100	C11H6O3	Phenylpropanoids	[M+H]+	pos	98264223150	MOL003590
4	Chrysin	4.6667	C15H10O4	Flavonoids	[M+H]+	pos	158026696.7	MOL002560
5	Salvigenin	5.9200	C18H16O6	Flavonoids	[M-H]-	neg	16781386.57	MOL002915
6	Liquiritin	5.3567	C21H22O9	Flavonoids	[M+H]+	pos	167494793.4	MOL004903
7	Isorhamnetin	5.5350	C16H12O7	Flavonoids	[M-H]-	neg	435247362.4	MOL000354
8	Formononetin	6.7283	C16H12O4	Flavonoids	[M-H]-	neg	4571298623	MOL010586
9	Lupiwighteone	7.8067	C20H18O5	Flavonoids	[M+H]+	pos	107096463	MOL003656
10	Costunolide	5.9683	C15H20O2	Terpenoids	[M+HCOO]-	neg	776729150.2	MOL010825
11	Glycyrrhizin	5.0050	C42H62O16	Terpenoids	[M-H]-	neg	988315071.7	MOL004876
12	Berberine	5.3000	[C20H18NO4]+	Alkaloids	[M+H]+	pos	4800455169	MOL001454
13	Kaempferol	5.5150	C15H10O6	Flavonoids	[M+H]+	pos	5041255402	MOL000422
14	Palmatine	5.6800	[C21H22NO4]+	Alkaloids	[M-NH3+H]+	pos	10984582594	MOL000785
15	Wogonin	0.5450	C16H12O5	Flavonoids	[M+H]+	pos	67163057.84	MOL000173
16	Glabranin	8.1300	C20H20O4	Flavonoids	[M+H]+	pos	3038143286	MOL004910
17	(-)-dehydrocostus lactone	5.2283	C15H18O2	Terpenoids	[M+H]+	pos	306314612	MOL001298
18	Atractylenolide iii	5.9883	C15H20O3	Terpenoids	[M+H]+	pos	788776509.2	MOL000181
19	Acacetin	5.8733	C16H12O5	Flavonoids	[M-H]-	neg	6381366350	MOL001689
20	Quercetin	5.8583	C15H10O7	Flavonoids	[M-H]-	neg	595853879.3	MOL000098
21	Astragaloside iv	6.3150	C41H68O14	Terpenoids	[M+HCOO]-	neg	19898885.61	MOL000409
22	Coptisine	6.1900	C19H14NO4+	Alkaloids	[M-NH3-H]-	neg	24070705.44	MOL001458
23	Naringenin	4.1567	C15H12O5		[M-H2O-H]-	neg	65274032.76	MOL004328
24	Moupinamide	3.9550	C18H19NO4		[M+H]+	pos	42965457.97	MOL008647
25	Baicalin	3.8950	C21H18O11		[M-H]-	neg	355673621.3	MOL002776
26	Medicarpin	6.9717	C16H14O4		[M+HCOO]-	neg	41161804.43	MOL002565
27	Vestitol	6.7233	C16H16O4		[M+HCOO]-	neg	9640128.732	MOL000500
28	Liquiritigenin	6.5833	C15H12O4	Flavonoids	[M+H]+	pos	184934778.1	MOL001792
29	Ononin	5.4533	C22H22O9		[M+H]+	pos	978433773.7	MOL000391
30	Caffeic acid	5.0950	C9H8O4	Phenylpropanoids	[M-H2O+H]+	pos	159036985.3	MOL000414
31	Vanillic acid	2.1500	C8H8O4	Phenols	[M-H2O+H]+	pos	64103985.47	MOL011357
32	Emodin	7.1950	C15H10O5	Quinones	[M+NH4]+	pos	36059070.69	MOL000472
33	Oroxindin	4.9283	C22H20O11	Flavonoids	[M-H]-	neg	27039148638	MOL013068
34	Alpinetin	6.3933	C16H14O4	Flavonoids	[M+H]+	pos	470157395.2	MOL000228
35	Scutellarein	5.2033	C15H10O6	Flavonoids	[M-H]-	neg	7249439 12.2	MOL002737
36	Luteolinidin	1.0967	C15H11O5+		[2M+H]+	pos	295429705.1	MOL001870
37	Palmitic acid	6.6000	C16H32O2	Fatty acids	[M-H]-	neg	267238648.9	MOL000069
38	Oleic acid	0.5967	C18H34O2	Organic acid	[M+H]+	pos	11293263.45	MOL000675
39	Jatrorrhizine	5.3383	[C20H20NO4]+	Alkaloids	[M+H]+	pos	420852024.6	MOL006397
40	Ferulate	7.3767	C10H10O4	Phenylpropanoids	[M+Na]+	pos	66824815.72	MOL000360
41	Chlorogenic acid	3.9017	C16H18O9	Phenylpropanoids	[M+H]+	pos	662237138.9	MOL001955
42	Magnoflorine	7.4050	C20H24NO4+	Alkaloids	[M-NH3+H]+	pos	1649353549	MOL000764
43	Columbamine	5.2383	C20H20NO4+	Alkaloids	[M+H]+	pos	964112673.1	MOL001457
44	Secoisolariciresinol	6.5383	C20H26O6	Phenylpropanoids	[M-H]-	neg	195722373.2	MOL001938
45	(+)-lariciresinol	7.4767	C20H24O6	Phenylpropanoids	[M+HCOO]-	neg	19426528.25	MOL000416
46	Luteolin	4.7950	C21H18O12	Flavonoids	[M+H]+	pos	1326534085	MOL000006
47	Scopoletin	5.7900	C10H8O4	Phenylpropanoids	[M+H]+	pos	170751598.7	MOL000040
48	Syringin	3.8550	C17H24O9	Phenylpropanoids	[M+NH4]+	pos	107014113.8	MOL000347
49	Myristic acid	7.0950	C14H28O2	Fatty acids	[M+H]+	pos	67530221.49	MOL001393
50	Apigenin	4.8000	C21H18O11	Flavonoids	[2M-H]-	neg	451939949.6	MOL000008
51	Isobavachin	7.3900	C20H20O4	Flavonoids	[2M-H]-	neg	215599847.4	MOL000448
52	Bergapten	5.4383	C12H8O4	Phenylpropanoids	[2M+H]+	pos	29716987.2	MOL001945
53	Geranyl acetate	4.8567	C12H20O2		[M+HCO3]-	neg	23281640.85	MOL000128
54	(+)-alpha-pinene	4.5700	C10H16	Terpenoids	[M+H]+	pos	332677731.4	MOL000485

(*Continued*)

https://doi.org/10.2147/JIR.S510966

Table 2 (Continued).

No.	Name	RT(min)	Formula	Class	Precursor_Type	pos/neg	Intensity	MOL ID
55	Techtochrysin	4.8517	C16H12O4	Flavonoids	[M-H]-	neg	145206860.1	MOL009356
56	(+)-trans-carveol	4.7333	C10H16O		[M+H]+	pos	328650005.1	MOL004709
57	Tricosanoic acid	7.6533	C23H46O2	Ketones, Aldehydes, Acids	[M-H]-	neg	124610694.9	MOL001993
58	Ellagic acid	0.5450	C14H6O8	Phenols	[M-H]-	neg	696303.2103	MOL001002
59	Cinnamaldehyde	1.4250	C9H8O		[M+NH4]+	pos	705637330.3	MOL000991
60	Hexanal	0.5967	C6H12O		[M+NH4]+	pos	9075104.038	MOL000666
61	Geranylacetone	5.0333	C13H22O		[M+H]+	pos	79588506.3	MOL000724
62	Beta-ionone	6.3317	C13H20O		[M+H]+	pos	131838330.9	MOL002363
63	(+)-beta-phellandrene	5.0667	C10H16	Terpenoids	[M+H]+	pos	46543036.94	MOL002028
64	Isoliquiritigenin	4.0267	C15H12O4	Flavonoids	[M+H]+	pos	113368137	MOL001789
65	Glycycoumarin	7.2383	C21H20O6	Flavonoids	[M-H]-	neg	622309838	MOL004878
66	Pinocembrin	4.7950	C15H12O4	Flavonoids	[M+H]+	pos	2890567797	MOL002844
67	Castanin	8.1350	C17H14O5	Flavonoids	[M+H]+	pos	128911808	MOL000467
68	Liquiritin apioside	5.1833	C26H30O13	Flavonoids	[M-H]-	neg	755870710.3	MOL004953
69	Rutin	1.3583	C27H30O16	Flavonoids	[M+HCOO]-	neg	55101348.83	MOL000415
70	Coumarin	0.7117	C9H6O2	Phenylpropanoids	[M-NH3+H]+	pos	451071644	MOL000431
71	Daidzein	4.5517	C15H10O4	Flavonoids	[2M+H]+	pos	215500252.8	MOL000390
72	Nicotinic acid	1.1350	C6H5NO2	Vitamin	[M+H]+	pos	659539726.4	MOL000421
73	Uridine	1.1817	C9H12N2O6		[M-H]-	neg	892498554.8	MOL000059
74	Eugenol	8.4300	C10H12O2	Phenylpropanoids	[M-H2O+H]+	pos	10040138.66	MOL000254
75	Salidroside	3.1233	C14H20O7	Phenols	[M+NH4]+	pos	31253594.95	MOL002929
76	Tyrosol	3.5517	C8H10O2	Phenols	[M-H]-	neg	5852216651	MOL002930
77	Hyacinthin	3.7783	C30H27O13+	Flavonoids	[M-NH3+H]+	pos	36674561.79	MOL000714
78	Pulegone	5.2767	C10H16O		[M+Na]+	pos	205202953.1	MOL001972
79	Danshensu	0.8917	C9H10O5	Phenols	[M-OH+H]+	pos	34887585.13	MOL007134

and analysis, above data were processed by Cytoscape 3.9.1 to construct a novel hub network. Using the CytoNCA plug-in in Cytoscape, the core targets were mined according to the values of Degree (DC, >30) or, DC>49, Betweenness (BC, >1072) and Closeness (CC, >0.46), and then the top 21 were selected to build a network map of core targets with Cytoscape (Figure 10c and d). The top five targets are EGFR, STAT3, SRC, AKT1, and HSP90AA1, which can be considered as key targets in the anti-UC pharmacological mechanism of QCHS_JPBS formula. GO enrichment analyses of the 44 intersecting genes (DC>30) identified earlier revealed that the targeted genes were associated with biological processes (such as response to hormone and enzyme-linked receptor protein signaling pathway), cellular components (such as membrane raft and perinuclear region of cytoplasm), and molecular functions (such as protein kinase binding and phosphotransferase activity) (Figure 10e). Finally, the results of KEGG found that JAK-STAT signaling pathway, Wnt signaling pathway and Calcium signaling pathway were closely related to UC (Figure 10f). Based on the network pharmacology analysis, the anti-colitis effect of QCHS_JPBS formula may involve the above pathway.

Discussion

Strategies for UC treatment are limited, and the current drug choices demonstrate shortcomings such as high recurrence rates and side effects, resulting in suboptimal efficacy.[20] These shortcomings underscore the urgent need for safer, multi-targeted therapeutic alternatives. However, TCM treatment for UC has the advantages of being multi-targeted, having fewer side effects, and having stable efficacy. QCHS_JPBS formula consists of nine types of Chinese herbal medicines, among which single herbs or ingredients (such as Huanglian, berberine) can significantly alleviate the symptoms of DSS-induced colitis.[21,22] In this research, the pharmacological roles of QCHS_JPBS formula in improving ulcerative colitis were systematically elucidated, which were manifested as weight recovery, decreased DAI score, inhibition of colon length reduction, and decreased histopathological score. This work not only elucidates the pharmacological foundation of

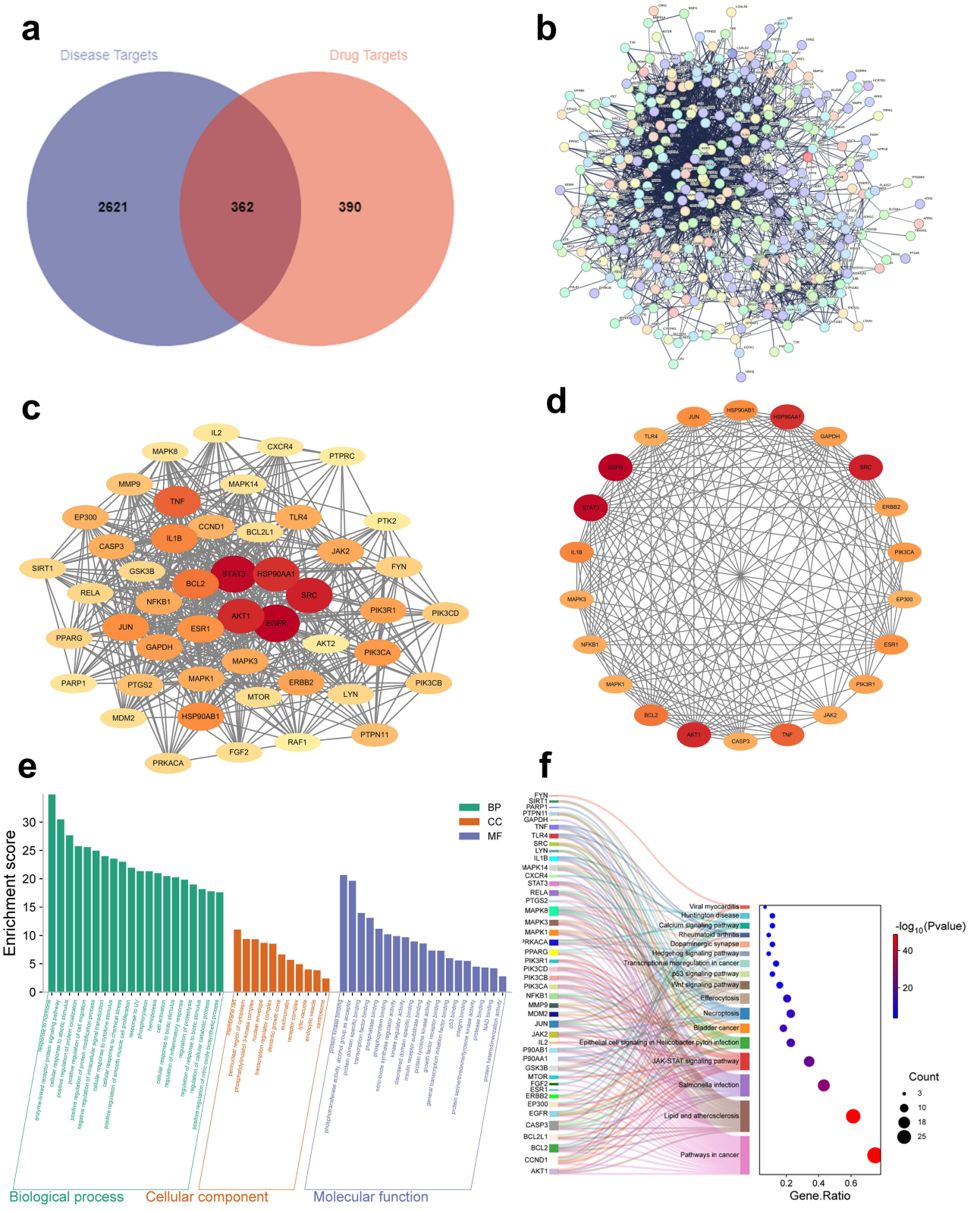

Figure 10 Network pharmacological analysis of the targets and pathways of QCHS_JPBS formula action. (**a**) Venn diagram of common targets of QCHS_JPBS formula and UC. (**b**) The PPI network analysis of core targets. (**c**) Hub-network extracted from the PPI network based on the degree value (>30). (**d**) Hub-network extracted from the PPI network of the top 21 targets based on the degree (>49), Betweenness (>1072) and Closeness (>0.46). (**e**) GO enrichment analysis for 44 key targets. (**f**) Sankey diagram for KEGG signaling pathway analysis.

https://doi.org/10.2147/JIR.S510966

QCHS_JPBS formula but also advances its translational potential as a clinically viable, multi-faceted therapeutic strategy for UC management.

The disruption of the intestinal epithelial barrier is an important pathological characteristic of UC. It is worth noting that the differentiation of ISCs is crucial for the repair of the intestinal epithelial barrier.[23] Specifically, various types of intestinal epithelial cells, such as goblet cells and intestinal endocrine cells, are derived from the proliferation and differentiation of ISCs to maintain intestinal mucosal regeneration and repair after injury.[24] In this study, QCHS_JPBS formula significantly promotes the differentiation of intestinal stem cells into goblet cells, which can secrete mucin to repair damaged intestinal mucosa. The proposal of these conclusions suggests that promoting the differentiation of ISCs may be an effective strategy for treating UC.

Increased evidence suggests that gut microbiota and its metabolites play a crucial role in the occurrence and development of UC, including regulating immunity, participating in signal transduction, and protecting the intestinal mucosal barrier.[25] On the one hand, UC patients exhibit characteristic changes in the diversity and abundance of gut microbiota compared to healthy individuals. Multiple bacteria were found penetrating the mucus layer in the intestinal tissue biopsy of UC patients.[26] The reduction of specific beneficial functional bacteria (such as *Bifidobacterium*) and the increase of potential pro-inflammatory and harmful pathogenic bacteria (such as *Enterococcus*) lead to dysbiosis of the gut microbiota.[27,28] The interaction between microbiota and intestinal mucosal immunity jointly induces an inflammatory environment in the intestinal cavity, leading to impaired intestinal barrier function.[29] In the present study, intervention with the QCHS_JPBS formulation reversed the DSS-induced increase in the abundance of *Clostridia* and *Lactobacillus* and decrease in the abundance of *Faecalibaculum* and *Muribaculaceae* in the feces of colitis mice. It is worth noting that the QCHS_JPBS formula intervention was able to elevate the relative abundance of *Akkermansia* genus, which has been shown to repair intestinal barrier function and thereby alleviate UC disease symptoms.[30] These results indicated that QCHS_JPBS formula was able to modulate gut microbiota disruption in DSS-induced colitis mice.

On the other hand, metabolites of gut microbiota also play an important role.[31] UC patients have reduced short-chain fatty acids (SCFAs), abnormal tryptophan metabolism, and increased inflammation-associated metabolites (such as free arachidonic acid and deoxycholic acid) in the gut.[32–34] In the DSS-induced colitis model, gavage administration of butyrate or indoleacrylic acid significantly improved UC disease symptoms in mice through mechanisms associated with the modulation of immunity and reduction of the inflammatory response.[35,36] In the present study, the intervention of QCHS_JPBS formula could reduce the relative level of sphingosine 1-phosphate and sphinganine, which are mainly related to the sphingolipid metabolism pathway. The accumulation of sphingosine-1-phosphate, an important mediator on this pathway, can impairs the intestinal barrier function and exacerbate colitis.[37] Therefore, QCHS_JPBS formula could restore metabolic imbalances in UC mice microbiota, thereby exerting anti-inflammatory effects.

Multiple microbial communities coexist and closely interact with ISCs in the intestinal.[38] Notably, metabolites are the bridge between the gut microbiota and ISCs interactions. The previously mentioned SCFAs have a promoting effect on ISC proliferation by inhibiting histone deacetylase activity.[39] Lactate, a bacterial metabolite, regulates ISC self-renewal by enhancing target gene expression in the Wnt/β-catenin pathway.[40] In addition, tryptophan is readily metabolized by the bacteria to a variety of biologically active amino acid derivatives. The latter can activate aryl hydrocarbon receptors and induce goblet cell differentiation in the gut, which is associated with the Notch and Wnt signaling pathways.[41,42] In the present study, FMT experiments showed that the bacteria intervened by the QCHS_JPBS formula promoted ISC differentiation and thus improved the symptoms of DSS-induced colitis. However, the metabolites that may be involved need to be further investigated.

Network pharmacology provides new perspectives and methods for the study of Chinese medicine compounding, which helps to deeply understand the multi-pathway and multi-target action characteristics of Chinese medicine.[43] In this study, network pharmacological analyses screened potential targets of QCHS_JPBS formula anti-UC, which included EGFR, STAT3, SRC, AKT1, and HSP90AA1. In addition, a number of signaling pathways were enriched, which included JAK-STAT signaling pathway, Wnt signaling pathway and Calcium signaling pathway. A multitude of evidence suggests that these targets and signaling pathways are closely related to the occurrence and development of UC.[44–46] Of course, the importance of the above targets or pathways in the anti-UC role of QCHS_JPBS formula should be appropriately and divinely examined in future studies, especially in the direction of ISC differentiation.

Conclusion

In summary, QCHS_JPBS formula promoted ISC differentiation, particularly in the direction of goblet cells, to repair the intestinal epithelial barrier of DSS-induced colitis. QCHS_JPBS formula also restored gut dysbiosis and regulated metabolic disorders in DSS-induced colitis mice. The conclusion drawn from the above experimental results is that QCHS_JPBS formula promotes the differentiation of ISCs through gut microbiota to repair the intestinal epithelial barrier in UC mice.

Data Sharing Statement

The data used to support the findings of this study are available from the corresponding author upon request.

Ethics Statement

All databases in this study are public databases, the contents of which are publicly available and allow unrestricted reuse through open licenses. According to official document issued by National Science and Technology Ethics Committee of China, the use of legally obtained public data is not subject to ethical scrutiny (https://www.gov.cn/zhengce/zhengceku/2023-02/28/content_5743658.htm). Therefore, the part of this study involving public databases would have the need for ethics approval waived (Ethics Committee in Affiliated Hospital of Nanjing University of Traditional Chinese Medicine). The animal studies were approved by the Animal Ethics Committee in Affiliated Hospital of Nanjing University of Traditional Chinese Medicine (Application Number: 2023DW-029-01) in accordance with the guidelines of the Guide for the Care and Use of Laboratory Animals.

Acknowledgments

This work was supported by the National Natural Science Foundation of China (82274483). Jiangsu Provincial Traditional Chinese Medicine Digestive Medicine Innovation Center (Su Health Science and Education Letter [2022] No. 15), Construction of high-level key disciplines of Traditional Chinese medicine (National TCM Human Education Letter [2023] No. 85), National Famous Old Chinese Medicine Expert Inheritance Studio (Chinese Medicine Teaching Letter [2022] No. 75).

Author Contributions

All authors made a significant contribution to the work reported, whether that is in the conception, study design, execution, acquisition of data, analysis and interpretation, or in all these areas; took part in drafting, revising or critically reviewing the article; gave final approval of the version to be published; have agreed on the journal to which the article has been submitted; and agree to be accountable for all aspects of the work. Yulai Fang and Shichen Min contributed equally to this work and share the first authorship. Hong Shen is the first corresponding author and Lei Zhu is the second corresponding author.

Disclosure

All authors have declared no conflict of interest.

References

1. Le Berre C, Honap S, Peyrin-Biroulet L. Ulcerative colitis. *Lancet*. 2023;402:571–584. doi:10.1016/S0140-6736(23)00966-2
2. Luo H, Cao G, Luo C, et al. Emerging pharmacotherapy for inflammatory bowel diseases. *Pharmacol Res*. 2022;178:106146. doi:10.1016/j.phrs.2022.106146
3. Hirten RP, Sands BE. New therapeutics for ulcerative colitis. *Annu Rev Med*. 2021;72:199–213. doi:10.1146/annurev-med-052919-120048
4. Yao D, Dai W, Dong M, Dai C, Wu S. MUC2 and related bacterial factors: therapeutic targets for ulcerative colitis. *EBioMedicine*. 2021;74:103751.
5. Mansouri P, Behmard E, Najafipour S, Kouhpayeh A, Farjadfar A, et al. Novel targets for mucosal healing in inflammatory bowel disease therapy. *Int Immunopharmacol*. 2025;144:113544.
6. Barbara G, Barbaro MR, Fuschi D, et al. Inflammatory and microbiota-related regulation of the intestinal epithelial barrier. *Front Nutr*. 2021;8:718356.
7. Okamoto R, Watanabe M. Role of epithelial cells in the pathogenesis and treatment of inflammatory bowel disease. *J Gastroenterol*. 2016;51:11–21.

8. Larabi A, Barnich N, Nguyen HTT. New insights into the interplay between autophagy, gut microbiota and inflammatory responses in IBD. *Autophagy*. 2020;16:38–51. doi:10.1080/15548627.2019.1635384
9. Zheng L, Duan S-L. Molecular regulation mechanism of intestinal stem cells in mucosal injury and repair in ulcerative colitis. *World J Gastroenterol*. 2023;29:2380–2396. doi:10.3748/wjg.v29.i16.2380
10. Luo H, Li M, Wang F, et al. The role of intestinal stem cell within gut homeostasis: focusing on its interplay with gut microbiota and the regulating pathways. *Int J Biol Sci*. 2022;18:5185–5206. doi:10.7150/ijbs.72600
11. Liu Y, Li B-G, Su Y-H, et al. Potential activity of traditional Chinese medicine against ulcerative colitis: a review. *J Ethnopharmacol*. 2022;289:115084. doi:10.1016/j.jep.2022.115084
12. Shen H, Zhang S, Zhao W, et al. Randomised clinical trial: efficacy and safety of Qing-Chang-Hua-Shi granules in a multicenter, randomized, and double-blind clinical trial of patients with moderately active ulcerative colitis. *Biomed Pharmacother*. 2021;139:111580. doi:10.1016/j.biopha.2021.111580
13. Zhu L, Hen H, Liu L, Gu PQ, Cheng JF, Zhang L, et al. Effect of jianpi bushen qingchang huashi recipe on proliferation of bone marrow mesenchymal stem cells]. *Zhongguo zhong xi yi jie he za zhi Zhongguo zhongxiyi jiehe zazhi =. Chin J Integr Tradit West Med*. 2016;36:191–195.
14. Wang K, Chen Q, Shao Y, et al. Anticancer activities of TCM and their active components against tumor metastasis. *Biomed Pharmacother*. 2021;133:111044. doi:10.1016/j.biopha.2020.111044
15. Luo -T-T, Lu Y, Yan S-K, et al. Network pharmacology in research of Chinese medicine formula: methodology, application and prospective. *Chin J Integr Med*. 2020;26:72–80. doi:10.1007/s11655-019-3064-0
16. Zheng S, Xue T, Wang B, Guo H, Liu Q. Application of network pharmacology in the study of mechanism of Chinese medicine in the treatment of ulcerative colitis: a review. *Front Bioinforma*. 2022;2:928116. doi:10.3389/fbinf.2022.928116
17. Zheng S, Liang Y, Xue T, et al. Application of network pharmacology in traditional Chinese medicine for the treatment of digestive system diseases. *Front Pharmacol*. 2024;15:1412997. doi:10.3389/fphar.2024.1412997
18. Wada H, Miyoshi J, Kuronuma S, et al. 5-Aminosalicylic acid alters the gut microbiota and altered microbiota transmitted vertically to offspring have protective effects against colitis. *Sci Rep*. 2023;13:12241. doi:10.1038/s41598-023-39491-x
19. Zhang Z, Zuo L, Song X, et al. Arjunolic acid protects the intestinal epithelial barrier, ameliorating Crohn's disease-like colitis by restoring gut microbiota composition and inactivating TLR4 signalling. *Phytomedicine*. 2024;123:155223. doi:10.1016/j.phymed.2023.155223
20. Liu J, Di B, Xu -L-L. Recent advances in the treatment of IBD: targets, mechanisms and related therapies. *Cytokine Growth Factor Rev*. 2023;**71**–**72**:1–12. doi:10.1016/j.cytogfr.2023.07.001
21. Li H, Fan C, Lu H, et al. Protective role of berberine on ulcerative colitis through modulating enteric glial cells-intestinal epithelial cells-immune cells interactions. *Acta Pharm Sin B*. 2020;10:447–461. doi:10.1016/j.apsb.2019.08.006
22. Xie Q, Li H, Ma R, et al. Effect of Coptis chinensis franch and Magnolia officinalis on intestinal flora and intestinal barrier in a TNBS-induced ulcerative colitis rats model. *Phytomedicine*. 2022;97:153927. doi:10.1016/j.phymed.2022.153927
23. Hou Q, Huang J, Ayansola H, Masatoshi H, Zhang B. Intestinal stem cells and immune cell relationships: potential therapeutic targets for inflammatory bowel diseases. *Front Immunol*. 2020;11:623691. doi:10.3389/fimmu.2020.623691
24. Wang Z, Qu Y-J, Cui M. Modulation of stem cell fate in intestinal homeostasis, injury and repair. *World J Stem Cells*. 2023;15:354–368. doi:10.4252/wjsc.v15.i5.354
25. Vestergaard MV, Allin KH, Eriksen C, et al. Gut microbiota signatures in inflammatory bowel disease. *United Eur Gastroenterol J*. 2024;12:22–33. doi:10.1002/ueg2.12485
26. Lawal SA, Voisin A, Olof H, Bording-Jorgensen M, Armstrong H. Diversity of the microbiota communities found in the various regions of the intestinal tract in healthy individuals and inflammatory bowel diseases. *Front Immunol*. 2023;14:1242242. doi:10.3389/fimmu.2023.1242242
27. Ni Y, Zhang Y, Zheng L, et al. Bifidobacterium and Lactobacillus improve inflammatory bowel disease in zebrafish of different ages by regulating the intestinal mucosal barrier and microbiota. *Life Sci*. 2023;324:121699. doi:10.1016/j.lfs.2023.121699
28. Balish E, Warner T. Enterococcus faecalis induces inflammatory bowel disease in interleukin-10 knockout mice. *Am J Pathol*. 2002;160:2253–2257. doi:10.1016/S0002-9440(10)61172-8
29. Amoroso C, Perillo F, Strati F, et al. The role of gut microbiota biomodulators on mucosal immunity and intestinal inflammation. *Cells*. 2020;9:1234. doi:10.3390/cells9051234
30. Zheng M, Han R, Yuan Y, et al. The role of Akkermansia muciniphila in inflammatory bowel disease: current knowledge and perspectives. *Front Immunol*. 2022;13:1089600. doi:10.3389/fimmu.2022.1089600
31. Zheng L, Wen X-L, Duan S-L. Role of metabolites derived from gut microbiota in inflammatory bowel disease. *World J Clin Cases*. 2022;10:2660–2677. doi:10.12998/wjcc.v10.i9.2660
32. Lavelle A, Sokol H. Gut microbiota-derived metabolites as key actors in inflammatory bowel disease. *Nat Rev Gastroenterol Hepatol*. 2020;17:223–237. doi:10.1038/s41575-019-0258-z
33. Hu Y, Chen Z, Xu C, Kan S, Chen D. Disturbances of the gut microbiota and microbiota-derived metabolites in inflammatory bowel disease. *Nutrients*. 2022;14:5140. doi:10.3390/nu14235140
34. Agus A, Planchais J, Sokol H. gut microbiota regulation of tryptophan metabolism in health and disease. *Cell Host Microbe*. 2018;23:716–724. doi:10.1016/j.chom.2018.05.003
35. Wlodarska M, Luo C, Kolde R, et al. indoleacrylic acid produced by commensal peptostreptococcus species suppresses inflammation. *Cell Host Microbe*. 2017;22:25–37.e6. doi:10.1016/j.chom.2017.06.007
36. Shin Y, Han S, Kwon J, et al. Roles of short-chain fatty acids in inflammatory bowel disease. *Nutrients*. 2023;15.
37. Argollo M, Furfaro F, Gilardi D, et al. Modulation of sphingosine-1-phosphate in ulcerative colitis. *Expert Opin Biol Ther*. 2020;20:413–420. doi:10.1080/14712598.2020.1732919
38. Markandey M, Bajaj A, Ilott NE, et al. Gut microbiota: sculptors of the intestinal stem cell niche in health and inflammatory bowel disease. *Gut Microbes*. 2021;13:1990827. doi:10.1080/19490976.2021.1990827
39. Farhadipour M, Arnauts K, Clarysse M, et al. SCFAs switch stem cell fate through HDAC inhibition to improve barrier integrity in 3D intestinal organoids from patients with obesity. *iScience*. 2023;26:108517. doi:10.1016/j.isci.2023.108517
40. Lee Y-S, Kim T-Y, Kim Y, et al. Microbiota-derived lactate accelerates intestinal stem-cell-mediated epithelial development. *Cell Host Microbe*. 2018;24:833–846.e6. doi:10.1016/j.chom.2018.11.002

41. Mar JS, Ota N, Pokorzynski ND, et al. IL-22 alters gut microbiota composition and function to increase aryl hydrocarbon receptor activity in mice and humans. *Microbiome*. 2023;11:47.
42. Wisniewski PJ, Nagarkatti M, Nagarkatti PS. Regulation of intestinal stem cell stemness by the aryl hydrocarbon receptor and its ligands. *Front Immunol*. 2021;12:638725. doi:10.3389/fimmu.2021.638725
43. Zhao L, Zhang H, Li N, et al. Network pharmacology, a promising approach to reveal the pharmacology mechanism of Chinese medicine formula. *J Ethnopharmacol*. 2023;309:116306.
44. Moparthi L, Koch S. Wnt signaling in intestinal inflammation. *Differentiation*. 2019;108:24–32. doi:10.1016/j.diff.2019.01.002
45. Salas A, Hernandez-Rocha C, Duijvestein M, et al. JAK-STAT pathway targeting for the treatment of inflammatory bowel disease. *Nat Rev Gastroenterol Hepatol*. 2020;17:323–337.
46. Wang Y, Li J-X, Ji G-J, et al. The involvement of ca(2+) signal pathways in distal colonic myocytes in a rat model of dextran sulfate sodium-induced colitis. *Chin Med J*. 2016;129:1185–1192. doi:10.4103/0366-6999.181968